Association
European Atomic Energy Community — EURATOM
KFA - Kernforschungsanlage, Jülich

FUSION TECHNOLOGY 1982

Proceedings of the twelfth Symposium
13-17 September 1982

In Two Volumes

Volume 1

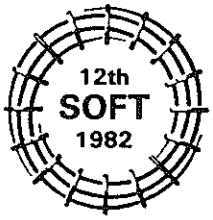

Published for the
COMMISSION OF THE EUROPEAN COMMUNITIES
by
PERGAMON PRESS
OXFORD • NEW YORK • TORONTO • SYDNEY • PARIS • FRANKFURT

DEMONSTRATION TOKAMAK POWER PLANT

M. Abdou, C. Baker, J. Brooks, D. Ehst, R. Mattas, and D. Smith
Fusion Power Program, Argonne National Laboratory
9700 S. Cass Ave., Argonne, IL 60439 U.S.A.
and
D. DeFreece, G. D. Morgan, and C. Trachsel
McDonnell Douglas Astronautics Company
P.O. Box 516, Bldg. 81/2, St. Louis, MO 63166

ABSTRACT

A design study of a tokamak-based fusion demonstration reactor was carried out. The study focused on four critical design features: 1) current drive for steady-state operation, 2) impurity control and exhaust, 3) breeding blanket, and 4) reactor configuration and maintenance.

1. INTRODUCTION

The objective of this study is to examine the critical issues for a tokamak-based demonstration (DEMO) power plant. The DEMO is the device that would follow the Fusion Engineering Device (FED) in the USA magnetic fusion program. Examining the fusion development strategy led to adopting several assumptions for the DEMO. A key assumption is that the DEMO does not need to produce economically competitive power. It needs only to demonstrate that an economically competitive system can be extrapolated.

The DEMO study /1/ was carried out by the STARFIRE /2/ team. Most of the effort was devoted to investigating the key issues for the DEMO that require extensive development in parallel to and beyond FED: 1) non-inductive current drive for steady-state operation, 2) impurity control and exhaust system, 3) breeding blanket, and 4) reactor configuration and maintenance. Furthermore, the strategy for R&D in these areas was examined. The detailed results of the study are documented in Reference 1. This short paper summarizes some of the important results.

The major reactor parameters for DEMO are shown in Table I. Areas of significant extrapolation from FED are the steady-state plasma burn, a power-producing tritium-breeding blanket, an increase in wall loading, and an increase in availability requirements.

2. CURRENT DRIVE

This section summarizes results from theoretical studies of a noninductive current drive for DEMO /1/. A lower hybrid (LH) system was previously designed in detail for STARFIRE /2/. The LH system appeared workable from an engineering and maintenance viewpoint, but accessibility constraints on the wave prevented wave penetration to the high-density plasma interior /3/. Hence, a survey of other drivers was conducted in order to identify those which more efficiently generate centrally peaked current density. The goal of our survey is to find which driver maximizes the net electrical power produced by the DEMO.

A large number of external drivers have been proposed which theoretically can sustain the toroidal tokamak current in a steady, noninductive state. Both plasma waves and particle beams have been suggested, and a survey of the most attractive candidates has been performed. We classify waves into three types. High-phase-speed (HS) waves are those which have toroidal phase velocities exceeding the electron thermal speed and which directly impart momentum to the circulating electrons. Examples of these waves, which have received experimental tests for driving current, are the lower-hybrid wave (JFT-2, PLT), the magnetosonic (Synchromak), and the ion-cyclotron wave (Model C). Low-phase-speed (LS) waves are those which have subthermal phase speeds and supply electron momentum. The most studied example is the fast wave, which is the compressional Alfven wave (CAW) at low frequencies and which is called a low-speed (short parallel wavelength) magnetosonic wave above the ion cyclotron frequency. The third wave-current-drive classification refers to ICRH and ECRH techniques, which heat plasma to create anisotropic resistivity, thereby indirectly driving currents. Beam-driven currents may be created by injection of neutral beams (DITE) or relativistic electron (REB) beams (SPAC-VI).

Table I. DEMO Major Parameters

Net Electric Power, MWe	390
Gross Electric Power, MWe	430
Fusion Power, MW	1069
Thermal Power, MW	1290
Gross Turbine Efficiency, %	33.6
Overall Availability	50
Average Neutron Wall Load, MW/m^2	2.1
Major Radius, m	5.2
Plasma Half-Width, m	1.3
Plasma Elongation (b/a)	1.6
Inboard Blanket/Shield Thickness (m)	1.2
Plasma Scrapeoff Thickness - Inboard (m)	0.2
Plasma Scrapeoff Thickness - Outboard (m)	0.165
Plasma Current, MA	8.68
Average Toroidal Beta	0.075
Toroidal Field on Axis, T	4.8
Maximum Toroidal Field, T	10
Number of TF Coils	8
Peak-to-Peak Field Ripple (Plasma Edge), %	3.5
Major Radius of TF Mid-Outboard Leg, m	11.6
Plasma Burn Mode	Continuous
Plasma Heating Method	Relativistic Electron Beam
Current Drive Method	Relativistic Electron Beam
Impurity Control	Pumped Limiter
Tritium Breeder	Li_2O
Breeding Ratio, Net	1.05
Maximum Component Weight, Mg	440
EF Coil System Stored Energy, GJ	5.66
TF Coil System Stored Energy, GJ	20.3

The driver power requirements have been compared on several levels: as the normalized current to power density ratio, j/p, as total current to power dissipated, I/P_{aux}, and as the net electric power, P_n, vs. plasma temperature. Here we summarize our findings and outline the logic which should be followed in order to identify the most attractive driver for the DEMO.

Figure 1 shows the $\hat{j}/\hat{p}$ plots for different wave types as a function of a common independent variable, v_d/v_e, where v_d is the parallel velocity associated with the driver. This quantity, v_d/v_e, is important, as it must be carefully chosen to maximize j/p. Our discussion here focuses on only a subset of all the drivers examined. Other drivers were rejected because of poorly developed theory, problems with experimental verification, or simply dismal prospects for achieving a reasonable DEMO driver. Starting with the neutral beam (D^0), we note from the figure that j/p has a well-defined maximum; fortunately, neutral beams have well-controlled energies so v_d can likely be selected to maximize j/p. A concern with this driver is that j/p may deteriorate by a factor of two if the neoclassical theory is inappropriate for some reason. Due to its similar physical current-drive process, ICRH results in j/p values similar to those from neutral beams. However, if minority ^3He is used, neoclassical theory predicts that j/p would be much less for $\varepsilon = 0.1$ than for $\varepsilon = 0$ (where ε is the reciprocal of the local flux surface aspect ratio), and that regions of reversed current density would also result. Furthermore, wave propagation and absorption determines the spatial variation of v_d/v_e; thus, it may be hard to arrange v_d/v_e so that $\hat{j}/\hat{p}$ is maximized.

The relativistic electron beam (REB) is the most efficient driver, if resistivity is greatly enhanced due to non-linear wave processes during pulsed injection. The dissipated power approaches the ohmic limit if v_d/v_e is properly chosen. Even if resistivity is not enhanced, the REB produces j/p values comparable with other drivers. Good control of v_d/v_e is easily achieved, and neoclassical effects are irrelevant for this driver. In the limit $v_d \to c$, LH has j/p identical to that of the REB (with $\alpha \equiv 1$), according to linear theory. In the strong heating limit ($D \equiv D^{QL}/D^{C} \gg 1$), the value of j/p about doubles for ECRH. However, in the limit $v_d < v_e$, there are indications that electron trapping may seriously degrade the efficiency of ECRH current drive. Moreover, it may prove difficult to

accurately launch rays which have one-sided damping (with $v_d >> v_e$) in order to maximize $\hat{j}/\hat{p}$. Additionally, there would be the necessity of developing high-power, high-efficiency sources of ECRH if this method were to prove practical for a DEMO.

As Figure 1 shows, the LH driver has $\hat{j}/\hat{p}$ values some 33% larger than those due to ECRH at $v_d > 3v_e$ in the linear regime. This is due to the wave-particle momentum transfer which accompanies the anisotropic heating. Neoclassical trapping strongly reduces j/p associated with the Landau damping of the LH driver when $v_d < v_e$; see the curve labeled LD. The principal defect with this driver, however, is the accessibility constraint inhibiting the generation of centrally peaked current profiles.

The low frequency ($\omega << \Omega_i$) limit of the fast wave is the CAW, which yields the largest $\hat{j}/\hat{p}$ values of all the waves when $\epsilon = 0$ and $v_d << v_e$. It is important to operate in the linear regime ($D << 1$), as this makes fullest advantage of the transit time damping mechanism, which yields the greatest j/p values. Neoclassical effects predominate when $v_d << v_e$, making predictions unreliable with this driver; hence, Figure 1 shows this curve dotted. Above the ion cyclotron frequency, the fast wave is referred to as the high speed magnetosonic (HSMS) wave when $v_d > v_e$. In this regime j/p values are seen to exceed those of the LH wave, which is due to the transit time damping mechanism. The HSMS has no accessibility constraint, and neoclassical trapping is of no concern.

An important parameter for the DEMO is the net power produced, P_n, which depends on the driver's power conversion efficiency, η_{aux}, and on the plasma temperature, $\bar{T}_e$; the fusion power, (P_f), and P_{aux} both vary with $\bar{T}_e$. For the DEMO, we desire 12 keV < $\bar{T}_e$ < 16 keV in order to keep the neutron wall load in the range ~ 1.5 MW/m^2-2.1 MW/m^2. Figure 2 epitomizes our results for three likely drivers. The neutral beam (3 MeV D°) is quite sensitive to η_{NB} -- an advanced electrostatic quadrupole-focused accelerator ($\eta_{NB} = 0.8$) yielding an acceptable $P_n > 100$ MW but an rf quadrupole-focused accelerator (with $\eta_{NB} = 0.35$) barely breaking even. (Negative ions with a photodetachment neutralizer are a necessary development which we assumed.) The HSMS (fast wave) is likewise sensitive to η_{aux}, but the system may need less development to achieve $\eta_{aux} = 0.7$ than the negative ion source neutral beam. For both the D° beam and the HSMS the 12 keV-16 keV range of $\bar{T}_e$ tends to maximize P_n at the desired wall loading, suggesting that the design is an optimum. The REB needs so little driver power that P_n is insensitive to η_{aux}. This is an advantage since it is often difficult to estimate η_{aux} accurately for current drive systems. The circulating power is so small for the REB that P_n peaks near the 8 keV maximum of P_f. However, the DEMO has a large thermal power (~ 1500 MW) at 8 keV; so the optimized design with the REB driver calls for a lower beta (than the 8% value used in Figure 2) with operation at 8 keV.

The selection of the best driver may now be considered in terms of engineering and equipment costs. Neutral beam lines introduce complexity into the reactor design, for tritium and neutrons are not well contained within the plasma chamber. In addition, neutral beams must be located within the reactor hall and will require fully remote maintenance. In contrast, the REB and HSMS systems have coaxial-transmission lines, which can conveniently be routed outside the reactor hall, and they incorporate vacuum windows. The vacuum windows in these structures assure good tritium containment, and the bends reduce radiation streaming. It is also desirable to select current drive systems which can simultaneously provide auxiliary heating to ignition during reactor startup. As shown in Reference 1, the REB system can be modified to operate at 20 Hz, yielding 80 MW of plasma heating during startup, and the system cost is estimated to be ~ $20 million (1981), exclusive of development costs. Results show that the HSMS system supplies over 80 MW of heating provided operation occurs at $\bar{T}_e$ < 18 keV; if we assume normal operation occurs at $\bar{T}_e$ = 18 keV, then about 80 MW of CW power is required. A cost analysis for this system has not been performed, but we note that similar current drive systems have been costed at $3.30 per watt delivered to the plasma, so an 80 MW system would cost ~ $264 million. Hence, the HSMS driver appears to be far more expensive than the REB. The couplers for the REB and the HSMS options have not been fully designed. Each has components inside the first wall, in the limiter shadow, and the engineering constraints may prove challenging.

The main concern with the REB is electron penetration; neoclassical orbits do not allow centrally peaked current density. Theoretical work on pulsed power injection for wave and neutral beam drivers is presently under way. Preliminary results suggest that the time-averaged $I/\langle P_{aux} \rangle$ could be increased modestly (by about factors of two to three), but a variety of difficulties appear which warrant further study.

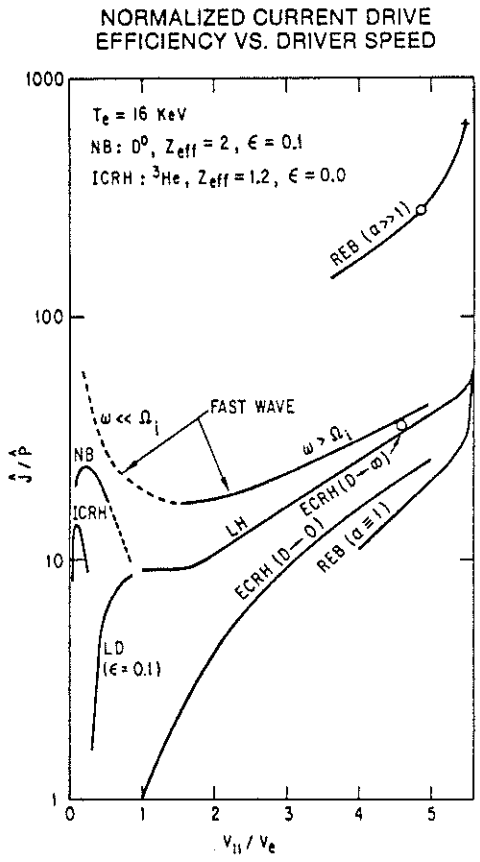

Fig. 1. Normalized current-density to power density ratio for various drivers. For pulsed REB injection, the return current and resistivity is enhanced by the factor α.

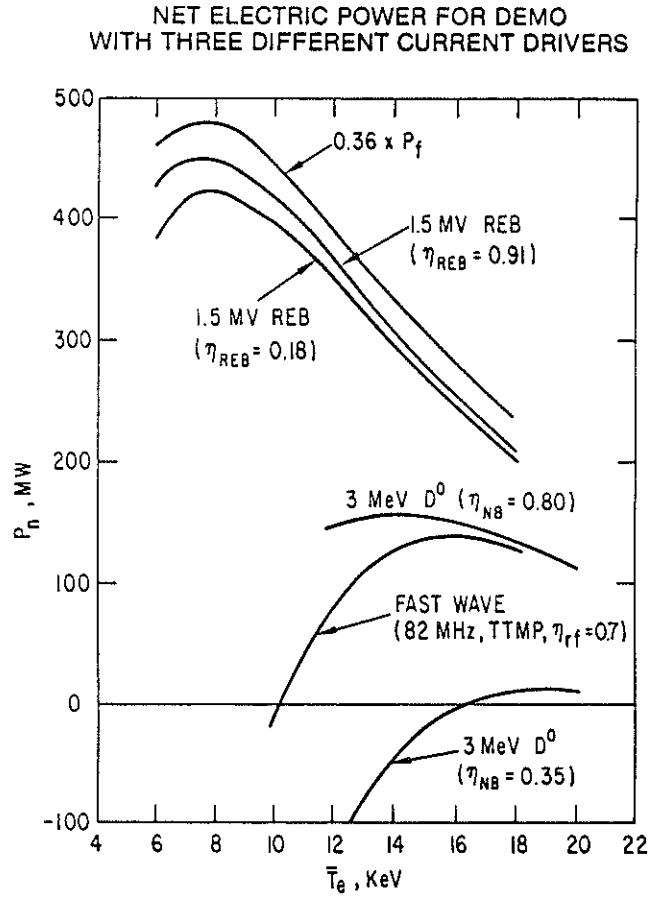

Fig. 2. Gross power (0.36 P_f) for DEMO reactor and net electric power for three driver candidates operating at different temperatures; R_o = 5.2 m and I = 9.01 MA. $P_n = (0.36\ P_f) - 22 - P_d\ (\eta_{aux})^{-1}$, in MW. For this survey $\bar{\beta}_t$ = 0.08 and B_o = 4.8 T.

3. BLANKET

The DEMO study focused on the definition of materials and design issues for first wall/blanket concepts using two different breeders: (1) solid lithium oxide (Li_2O) and; (2) a liquid metal, the lead-rich Li-Pb eutectic (17 at. % Li, 83 at. % Pb). Analyses related to materials selection, neutronics, tritium recovery, thermal-hydraulics and stress were performed, and critical design and operating criteria were defined for both concepts. In addition, the study addressed important aspects of first wall design which are generally insensitive to concept selection. These aspects included sputtering erosion, response to plasma disruptions, tritium permeation and nuclear response.

3.1 Li_2O breeder blanket concept

Pressurized water (260-300°C) was selected for the first wall and blanket coolant. The range of operating temperatures required for acceptable Li_2O performance is very limited, and thus the low ΔT characteristic of pressurized water systems appears necessary for a satisfactory design. Compared to helium coolant, water coolant permits a smaller reactor size or a higher fusion power provides for much lower pumping power losses, and results in lower cost of the heat transport system. An advanced austenitic stainless steel (designated PCA), similar to Type 316, was selected as the structural material. Mechanical properties and radiation damage resistance are considered acceptable for reasonable lifetimes (~ 7 MW-yr/m^2) at the relatively low projected operating temperatures, which are below the temperatures at which severe displacement damage embrittlement, helium embrittlement, and maximum swelling occur.

The 1-D neutronics calculations indicate that, in the absence of a neutron multiplier, the tritium breeding potential of a Li_2O blanket decreases significantly with ^6Li enrichment of natural lithium. The maximum breeding ratio (100% blanket) is 1.23 for a Li_2O blanket with a stainless steel first wall and armor 13.4-mm thick. However, the net breeding ratio (3-D) is only ~ 1.05 with no inboard blanket. Beryllium was found to be the only effective neutron multiplier for a Li_2O blanket. The beryllium multiplier is more effective when placed behind several centimeters of Li_2O. The physical properties, the thermodynamic properties, and the effects of radiation on the properties of Li_2O were evaluated in detail. Fabrication and handling problems associated with Li_2O were also assessed. Lithium oxide is very hygroscopic, reacting readily with moisture to form LiOH. Thus, high-purity Li_2O is difficult to produce and contamination during handling is a major problem. Recent investigations indicate that the solubility of LiOH in Li_2O is very low, and is expected to be less than 1 ppm in the reference blanket. Fabrication of Li_2O with small (< 4 μm) grain size and interconnected porosity, although difficult, appears feasible. However, the stability of this microstructure under anticipated thermal and radiation environments of a reactor blanket is a major concern. Large weight losses have been observed at 1000°C when Li_2O is exposed to vacuum or helium with very low moisture concentrations. This is generally attributed to mass transfer of LiOH. Also, chemical effects produced by burnup of lithium and displacement damage effects produced by energetic recoils of T and He are predicted to cause sintering and pore closure under certain conditions. Preliminary data indicate substantial restructuring of Li_2O after irradiation at temperatures > 750°C.

Tritium recovery is considered to be a key feasibility issue for Li_2O as a tritium breeder material. Tritium generated within the Li_2O grains must diffuse to the surface of the grains, desorb as T_2O, migrate through interconnected porosity to a helium purge stream, and connect to the tritium processing system. Similar to the case for STARFIRE, a Li_2O microstructure with small grain size (< 1 μm) and a bimodal pore distribution is believed to offer the greatest potential for acceptable tritium recovery. The difficult design problems arise from the limited operating temperature range projected for Li_2O and the relatively low thermal conductivity (about 4 W/m-K at 500°C for unirradiated material at 70% of theoretical density). Effects that result in a projected allowable operating temperature range between 410 and 670°C for Li_2O are summarized in Table II. The critical concerns relate to the fact that some of the phenomena may cause irreversible propagating-type effects. For example, precipitation of LiOT could lead to enhanced sintering at low temperatures, which, in turn, would produce higher tritium partial pressures and, hence, more LiOT precipitation and subsequently more sintering. Mass transport of LiOT leads not only to a loss of lithium from the blanket but also to possible corrosion problems caused by precipitation of liquid LiOT in the tritium processing circuit. Analyses indicate that, in the absence of radiation effects, the blanket tritium inventory can be maintained at relatively low levels (< 50 g in Li_2O). However, radiation effects are expected to substantially increase the tritium inventory, possibly to unacceptable levels.

Table II. Basis for Allowable Operating Temperature Range of Li_2O

Maximum Allowable Temperature	
Radiation-induced sintering	700°C
Mass Transport of LiOH (1% of T_2O)	670°C
Minimum Allowable Temperature	
Solid state diffusion (1 μm grain)	410°C
LiOT precipitation (160 Pa)	410°C

Materials compatibility issues include breeder-structure, coolant-structure and breeder-coolant compatibility. The first two issues involve normal operation whereas breeder-coolant compatibility is of interest only in the event of off-normal conditions such as a coolant leak into the breeder region. Limited data from short-term sealed capsule experiments indicate that the reactivity of Li_2O with stainless steel is probably not excessive. However, no data exist under the more severe conditions of appropriate oxygen and moisture pressures. The potential for stress corrosion cracking of cold-worked austenitic steel under attainable conditions in the presence of tritium or hydrogen requires further investigation. Likewise, detailed analyses must be conducted to assess the severity of a breeder-coolant reaction that would result from a coolant tube leak.

Thermal-hydraulics analyses were conducted to evaluate the sensitivity of the blanket design, particularly with respect to tritium recovery, to variations in breeder physical properties, geometrical parameters, and reactor power level. The results indicated that the tolerances required for adequate predictability of heat transfer through a helium gap at the breeder-to-coolant-tube interface were too small a practical system. A different design concept, which has been considered for the interface, consists of a commerical stainless steel metallic felt between the breeder and tube. The thermal conductance of the interface can be adjusted by varying the thickness and density of the felt. The blanket was also analyzed to determine the design changes necessary to accommodate deliberate large-scale changes in reactor power level. A power factor change of 2 could potentially be accommodated by making design detail changes, which would result in a reduction of ~ 0.08 in tritium breeding ratio. Thermal stress analyses of the Li_2O breeder were conducted to determine the breeder's propensity to fracture under operational thermal gradients (410°C to 660°C radially outward from the cylinder's central coolant tube, over a 2 to 6 cm cylinder diameter). Circumferential and axial stresses in the cylinder were higher by factors of 4 to 8 than the reported fracture strength level. Breeder cracking, if it occurs, will change the blanket configuration and hence increase the difficulty in predicting breeder performance during operation. The cracks themselves are additional interfaces which, if unfavorably oriented, can increase the impedance to heat flow and thereby result in temperatures higher than the allowable maximum. Since the primary heat flow is in the radial direction, the formation of circumferential cracks that impede radial heat flow is not likely. Radial and axial cracks, on the other hand, do not represent large barriers for radial heat conduction, even though the local temperatures will be influenced by the heat-transfer medium existing between the crack faces. The most undesirable effect of cracking appears to be the difficulties created in controlling thermal conductance at the breeder-to-tube interface. Similar to UO_2 and/or $(U,Pu)O_2$ nuclear fuels, Li_2O breeder may fracture into fragments and thus greatly complicate the thermal conductance control. The impact of breeder cracking on the flow characteristics of the helium purge stream is also an important consideration. Of the critical Li_2O properties that affect cracking, fracture strength and Young's modulus, in particular, warrant experimental investigation.

The reference Li_2O breeder first wall/blanket design is illustrated in Figure 3. Major parameters are listed in Table III, and key features of the design are shown in Table IV. The first wall and blanket are integrated mechanically and structurally into modules, assembled into eight blanket sectors, identical except for local variations required for other reactor components (e.g., REB current drive launcher). The first wall is a beryllium-clad corrugated panel, with channels of circular segment cross section. The breeder and first wall are cooled by high-pressure (11.0 MPa), high-temperature (260°C inlet, 300°C outlet) water. The breeder coolant is contained in small-diameter tubes connected to inlet

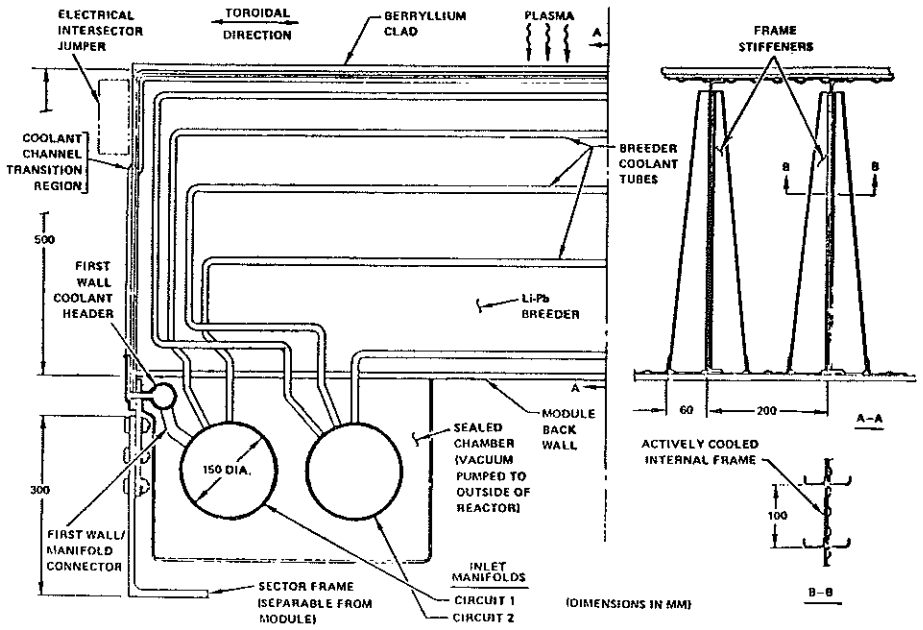

Fig. 3. Li_2O Solid Breeder First Wall/Blanket Design

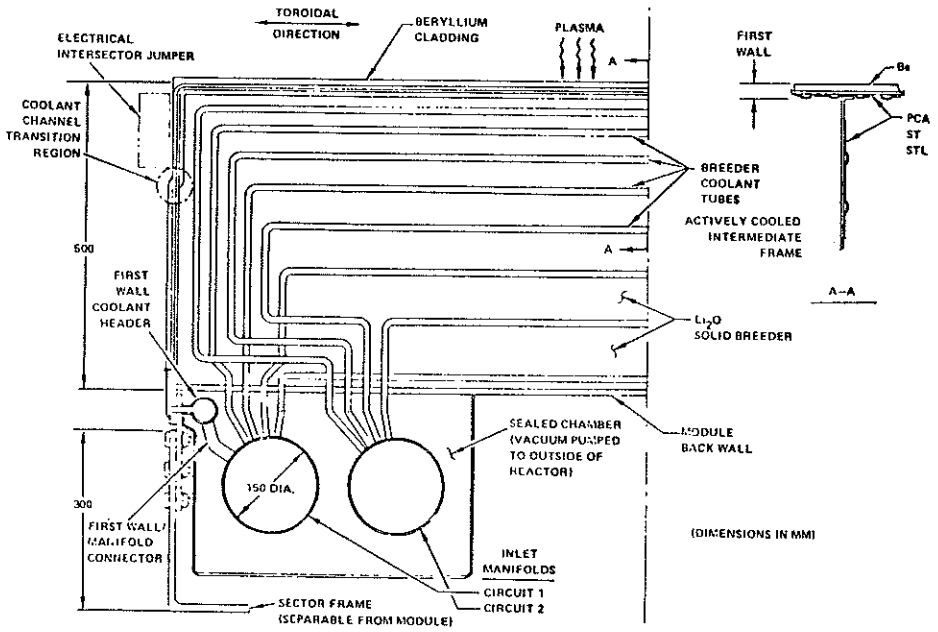

Fig. 4. 17Li-83Pb Liquid Alloy Breeder First Wall/Blanket Design

Table III. Li_2O Breeder Reference First Wall/Blanket Concept Description

Selected Materials	
- Tritium Breeder	Li_2O (solid; 70% TD)
- Coolant	Pressurized H_2O (11.0 MPa) - Inlet temperature 260°C - Outlet temperature 300°C
- Tritium Processing Fluid	Low-velocity Helium (0.05 MPa)
- Structure	Modified Austenitic Stainless Steel
Selected Design Options	
- First Wall	Be-clad Corrugated Panel
- Breeder Coolant Containment	Small-diameter Tubes
- Other:	
- First wall and blanket mechanically and structurally integrated	
- Coolant flow in toroidal direction	
- Dual parallel primary coolant loops	
- Maintenance by sector removal and replacement	

Table IV. Key Features of Selected Design Details for Li_2O Solid Breeder Reference First Wall/Blanket Concept

First Wall: Be-clad Corrugated Panel

- Minimum number of pressure boundary welds
- Separates structural and surface-related requirements
- All plasma chamber components coated with same material (Be)
- Low structure temperature (< 400°C)
- Mechanically and structurally integrated with blanket

Breeding Zone: Sintered Ceramic with Coolant in Tubes

- All tube pressure boundary welds located outside of breeder zone in low fluence region
- High pressure coolant contained in small-diameter tubes
- Coolant tubes oriented toroidally
- Tube spacing graded to conform to energy deposition profile
- Reduced density ceramic (70% TD with bi-modal porosity) to facilitate tritium recovery
- Low pressure He purge stream for tritium recovery
- Coolant outlet temperature and pressure reduced (from STARFIRE) to increase reliability

Manifold Zone: Tubular Manifolds

- Most coolant system welds located within vented secondary containment to accommodate minor leakages while reactor continues to operate
- Steel and water, together with shield, serve as neutron reflectors

Dual Independent Primary Coolant Loops

- Dual loops throughout each module and sector to provide adequate afterheat removal even if only one loop is operable

and outlet manifolds at the rear of the blanket. A stainless steel metallic felt, which accommodates thermal expansion differences between the breeder and tube and conducts the heat from the breeder to the tube is being evaluated for control of the breeder temperature. The Li_2O breeder is fabricated at 70% of theoretical density, with bimodal porosity to enhance tritium release. Helium purge gas at approximately 1 atm flows through 2-mm diameter holes in the breeder to remove tritium. Dual parallel primary coolant loops are provided to effect safe removal of afterheat in the event of a coolant circuit failure. Maintenance of the first wall/blanket is performed by sector removal and replacement, to minimize downtime.

3.2 Li-Pb alloy blanket concepts

Liquid Li-Pb alloys have several attractive properties for use as a tritium breeder in a fusion reactor, viz., excellent tritium breeding performance and acceptable tritium recovery characteristics. The 17Li-83Pb eutectic alloy, which has a relatively low melting temperature, 235°C, was selected as the reference breeding material for the liquid breeder portion of the DEMO blanket study.

The most important initial consideration for the blanket design is whether to use Li-Pb as both breeder and coolant (i.e., self-cooled), or to use a separate gas or liquid coolant. Economics-related issues (e.g., pumping power losses and energy-conversion-efficiency), safety, and blanket and coolant system design complexity are of primary concern. The most important materials-related concerns pertinent to the design evaluations are: (1) the high density of Li-Pb, which increases blanket structural requirements (and pumping power requirements if used as a coolant); (2) the maximum allowable structural temperature, set at ~ 400°C for ferritic steel because of compatibility concerns; and (3) the low solubility of tritium in Li-Pb, which impacts both tritium containment and tritium recovery. For separate coolant concepts, additional important design considerations are breeder-coolant compatibility, control of tritium permeation into the coolant, breeder containment approach, and coolant containment approach (e.g., fully pressurized module or small-diameter coolant tubes). Induced magnetohydrodynamic (MHD) effects are also important concerns for Li-Pb breeder self-cooled concepts and for separately cooled concepts using liquid metal coolant (i.e., sodium).

Helium, pressurized water, and liquid sodium have been considered as potential coolants for the separate-coolant concepts. Sodium, on balance, is considered to be the best separate coolant, primarily because of its good thermal-hydraulic characteristics, its low reactivity with Li-Pb, and its potential to serve as a tritium-recovery medium without requiring Li-Pb circulation. However, MHD effects and reactivity of sodium with water and air are major concerns.

Compatibility of Li-Pb with structural materials is a key feasibility question. The maximum blanket operating temperature was limited by corrosion/compatibility criteria. Critical issues include (1) corrosion/mass transfer effects and (2) stress corrosion effects. Ferritic steel and vanadium alloys are considered to be the best candidates for the structural material. Because of the high solubility of nickel in both lithium and lead, structural alloys containing significant amounts of nickel are subject to extensive mass transfer at high temperatures. Corrosion of austenitic steels in a large heat transport system is believed to be excessive at acceptable operating temperatures (> 400°C). Those ferritic steels with no nickel should be more resistant to mass transfer effects; however, liquid metal embrittlement at low temperatures (~ 350°C) is of concern for structures under high stress. Vanadium alloys probably have better compatibility with Li-Pb because of lower solubilities in lithium and lead; however, no experimental data are available. Also, for separately cooled concepts compatibility of structure with the separate coolants is a major consideration.

Neutronics analyses for the Li-Pb breeder blanket indicate that breeding ratios of ~ 1.5-1.6 (1-D basis) are attainable for blankets at 100% coverage and 70-cm depth, depending on first wall materials and thicknesses. However, the Li-Pb must be highly enriched, to ~ 60-70% of ^6Li, to achieve these breeding ratios. A Li-Pb blanket with natural lithium will provide a breeding ratio of only 1.2-1.3 for otherwise similar conditions.

Key properties of 17Li-83Pb that have major impact on the blanket design include its melting temperature (235°C), relatively high density (9.4 g/cm^3), and relatively low solubility for hydrogen (tritium). For a relatively high tritium pressure of 1 Pa, the amount of tritium dissolved in the alloy is only about 4.4 wppb at projected operating temperatures. This low solubility has important implications regarding tritium recovery,

tritium inventory, and tritium containment. At this pressure, tritium permeation rates are quite high for most structural materials. The heat of reaction of the 17Li-83Pb alloy with air and water is lower than that of liquid lithium by a factor of ten when compared on a unit volume basis.

Tritium recovery and containment problems were evaluated for both self-cooled and separately cooled concepts. Because of the low solubility of tritium in 17Li-83Pb, fairly high tritium pressures (about 1 Pa) are required to attain acceptable flow rates if Li-Pb is used as the tritium recovery fluid. These high tritium pressures create tritium containment difficulties for self-cooled concepts in the "ex-reactor system", e.g., the steam generator and piping. An intermediate heat exchanger or a double-walled steam generator would be required to reduce leakage of tritium to acceptable levels. Molten salt extraction, the use of solid getters, and gas sparging are considered feasible methods for direct recovery of tritium from Li-Pb. For sodium coolant in the separately cooled concept, permeation rates into the sodium appear to be sufficient to use the sodium as the tritium recovery fluid. Cold-trapping is the most attractive method for recovery of tritium from the sodium.

The sodium-cooled Li-Pb first wall/blanket concept is illustrated in Figure 4; major parameters are listed in Table V. The module/sector approach used for the Li_2O breeder blanket was adopted for this Li-Pb breeder blanket concept. The first wall and blanket are integrated mechanically and structurally. The first wall consists of a beryllium-clad corrugated panel. The breeder zone and first wall are cooled by low-pressure ($\lesssim$ 1 MPa), high-temperature (275° inlet, 400°C outlet) liquid sodium, contained in small-diameter toroidally oriented tubes which are connected to inlet and outlet manifolds at the rear of the blanket. Tritium permeates from the Li-Pb (which does not circulate out of the modules) through the coolant tube walls into the sodium; a small percentage of the sodium flow is processed externally by cold trapping to remove the tritium.

For the Li-Pb self-cooled first wall/blanket concept, the beryllium-clad first wall of each module is formed by two semi-ellipsoidal domes which comprise the module front face. The flat side walls of the module are connected to full internal frames (oriented normal to the toroidal direction) which self-react loads due to internal pressure ($\sim$ 1-2 MPa). The frames also react the gravity loads of the Li-Pb from the side walls and first wall (depending on module location in the sector) to the back wall and sector structure. The Li-Pb enters the rear of the blanket at about 300°C, flows to the front of the blanket through radial feedpipes, and is channeled directly behind the first wall to cool it. The liquid metal then circulates at a lower velocity toward the back of the blanket, and exits at 400°C to the outlet manifold. A fraction of the Li-Pb flow is diverted to an ex-reactor tritium processing system for tritium recovery.

Table V. DEMO Li-Pb Liquid Metal Alloy Breeder Blanket Description

Selected Materials	
- Tritium Breeder	Liquid 17Li-83Pb Alloy
- Coolant	Liquid Sodium ($\lesssim$ 0.5 MPa) - Inlet temperature $\sim$ 275°C - Outlet temperature $\sim$ 400°C
	Ferritic Steel or Vanadium Alloy
Selected Design Options	
- First Wall	Be-clad Corrugated Panel
- Breeder Coolant Containment	Small-diameter Tubes
- Other:	
- Toroidal direction for coolant flow	
- Dual parallel primary coolant loops	
- Maintenance by sector removal and replacement	

4. REACTOR CONFIGURATION

An area of major uncertainty is the ability of the reactor to achieve its availability goal, which is dependent on component outage rate (reliability and lifetime) and on the

outage time for maintenance (replacement time). Confidence in the data base for reactor component reliability and life will be low because extended testing will not be possible prior to DEMO. As a result DEMO will have features which enhance reliability and minimize replacement time. The most important design feature selected to enhance reliability is steady-state plasma operation, which reduces cyclic loading and minimizes the number of plasma disruptions. Another important aspect in the DEMO is that availability will be improved by striving for reactor simplicity. Since the STARFIRE study, the INTOR group has shown the feasibility of utilizing a 4°K anti-torque structure, which greatly improves access to the reactor. This feature was incorporated into the DEMO design.

The DEMO reactor design was further simplified by reducing the number of components and connections, simplifying sealing surface geometry, and combining components to reduce the number of maintenance operations required (saves time) and decrease complexity (improves reliability). The major configuration features that lead to reactor simplification are: a) a 4°K anti-torque structure, b) one limiter/blanket/shield sector per TF coil, c) eight TF coils, d) a combined TF coil and plasma boundary, and e) a segmented anti-torque structure. These features have resulted in a decrease in the number of major parts by a factor of two from the STARFIRE configuration and reduced the number of major seals and connections by a factor of four.

The configuration selected for DEMO is shown in the cross-section view of Figure 5 and in the isometric view of Figure 6. Dominant features of the configuration are the flat top on the reactor, which was chosen to minimize the reactor building height; the single sector per TF coil; and the combined vacuum boundary with sector sealing near the outer leg of the TF coil. No intertwined superconducting coils are used and four sets of redundant vacuum pumps are located in the basement.

One blanket/shield/limiter sector per TF coil was chosen for DEMO after evaluation of its effect on availability and stored energy. The number of maintenance operations required for replacement and the relative reliability of that configuration were compared to a configuration using two sectors per TF coil. It was found that the number of seal connections was reduced by a factor of four and the number of major components requiring replacement was reduced by a factor of two. These changes reduce the replacement time by approximately a factor of two and increase the blanket system reliability by as much as a factor of four (if connections dominate the reliability, as expected).

Choice of a single, blanket/shield/limiter sector per TF coil results in the need for a larger TF coil outer leg radius so that adequate access is provided for single sector installation. The outer leg radius and peak-to-peak field ripple are 11.6 m and 3.5% for 8 coils, 12 m and 1.1% for 10 coils, and 12.3 m and 0.3% for 12 coils. Eight TF coils were chosen to minimize the reactor size and, because the number of blanket/shield/limiter sectors is proportional to the number of TF coils, to reduce the number of connections and major components, further reducing replacement time and increasing reliability.

The decision of one sector per TF coil increased the requirements for TF coil size and, consequently, the stored energy in the EF coil system and the reactor building size. These effects were evaluated to determine the increased capital costs. A study of the EF coil stored energy indicated that the major benefit could be obtained by decreasing the TF coil height (~ 6 GJ/m), as opposed to decreasing the TF coil radius (~ 0.5 GJ/m). As a result, a curvature-supported TF coil shape was selected in place of the conventional coil shape. The curvature-supported coil requires an extension of the center post at the top and bottom of the coil inner leg to maintain a pure tension coil. The building height was not affected by the coil radius change and the additional costs for building width was ~ $10M. These costs are not considered excessive compared to the benefits derived in availability.

Simplified TF coil replacement was achieved by eliminating the need for a common vacuum tank around the inner legs of the TF coils and by adopting the 4°K anti-torque structure of INTOR. It was found that, if the basic vacuum boundary was moved to the exterior of all TF and EF coils and the shield sectors were inserted through this boundary and sealed together under each TF coil, then separate vacuum boundaries could be provided for the plasma and TF coils using all planar seals. These seals are inherently simpler to replace than the structural joints used in the common vacuum tank of previous designs, where structural welds had to be cut and remade. Dual seals with intermediate vacuum pumping between shield sectors limit tritium leakage. Additionally, the 4°K anti-torque structure was segmented with a clevis joint equidistant between the coils to permit carrying the overturning load without structural welding. This segmentation permits radial coil removal after the blanket and shield sectors, outer EF coils, and the outer vacuum wall panel are removed. Another

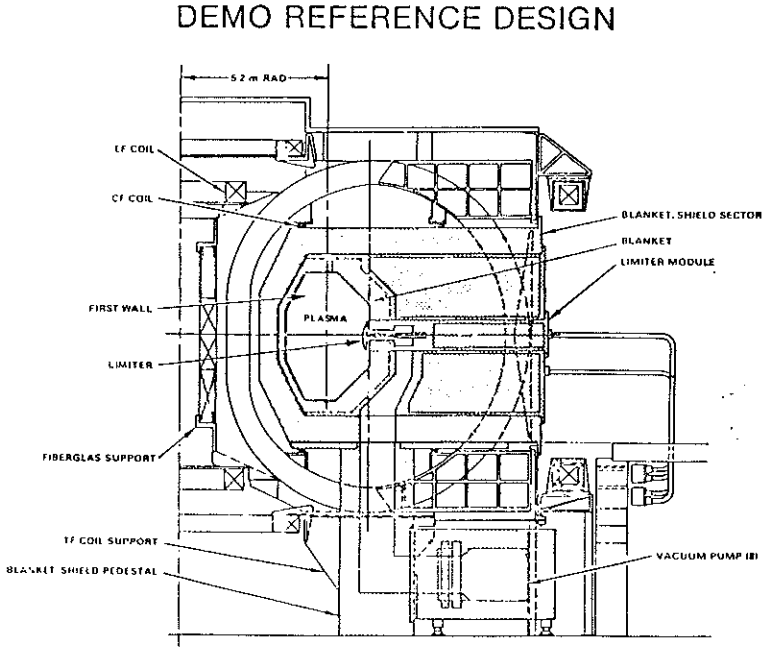

Figure 5.

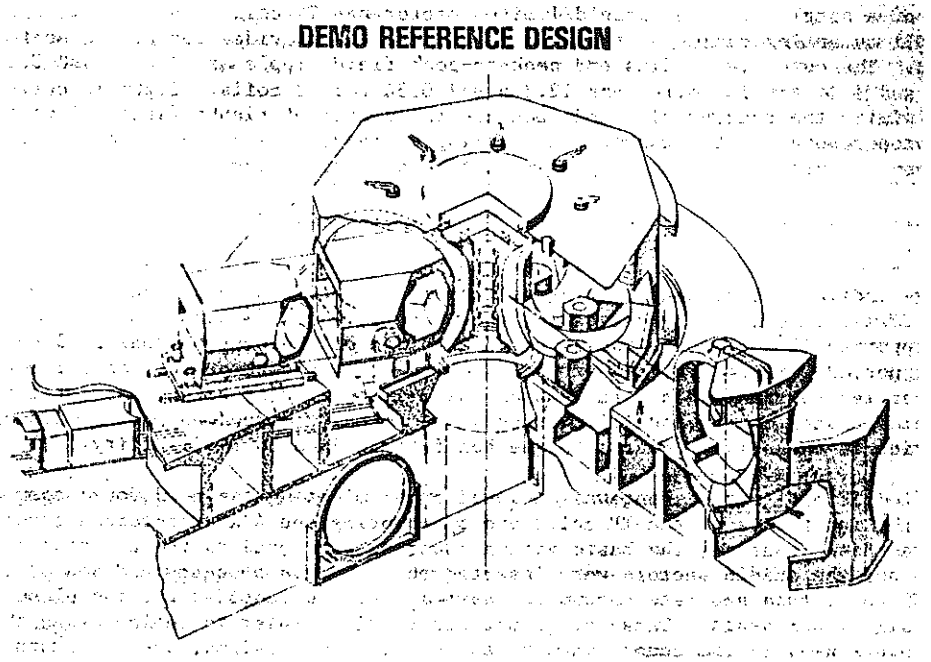

Figure 6.

major benefit of the combined vacuum boundary is that it eliminates the need for an additional structural boundary between the TF coils and the shield. This results in eliminating ~ 8 cm of radial build in the inner blanket/shield and could result in capital cost savings of ~ $50M. Yet another benefit of the combined vacuum boundary is that all magnetic loads in the 4°K structure can be reacted without additional thermal isolation. The large outer EF coils are supported by the 4°K TF coils, and the inner EF coils are supported by the center post.

All structure at 4°K is supported by fiberglas epoxy compression pads under each TF coil. These pads also support the center post. The vacuum loads on the flat top/lid of the reactor are transmitted to the 4°K structure through fiberglass epoxy compression pads to save reactor building height without significant 4°K heat loss.

TF coil replacement is accomplished by removing the blanket/shield sectors on either side of the coil, removing the outer EF coils and vacuum tank rings, cutting the outer wall panel and extracting the coil radially. It is estimated that TF coil replacement can be achieved in less than six months using remote maintenance with this approach. This represents an improvement of a factor of at least two over previous designs.

Previous designs incorporated lower EF coils that were trapped under the reactor and provided in-place spares for recovery in event of coil failure. The DEMO design has provisions for direct replacement of these lower coils through a pit and tunnel.

It is believed that DEMO has reactor-related design features that should permit it to achieve an acceptable availability and that should lead to an attractive commercial reactor.

REFERENCES

/1/ ABDOU, M. A., et al., "A Demonstration Tokamak Power Plant Study," ANL/FPP/TM-154, Argonne National Laboratory (March 1982).

/2/ BAKER, C. C., et al., "STARFIRE - A Commercial Tokamak Fusion Power Plant Study," ANL/FPP-80-1, Argonne National Laboratory (September 1980).

/3/ EHST, D., "Driver Options for Steady State Tokamaks," Proceedings of the IEEE 9th Symposium on Engineering Problems of Fusion Research, IEEE Publication No. 81CH1715-2 NPS (1981).